Granular Matter (2011) 13:159–168
DOI 10.1007/s10035-010-0222-7

# Particle velocity profiles and residence time distribution in mixed-flow grain dryers

**Kingsley Lawrence Iroba · Jochen Mellmann · Fabian Weigler · Thomas Metzger · Evangelos Tsotsas**

Received: 9 March 2010 / Published online: 30 September 2010


**Abstract** Non-uniform moisture content distribution of grains at the discharge of Mixed-Flow Grain Dryers is one of the sources of product quality loss during subsequent storage. Unfavorable design of this kind of dryers may cause uneven residence times of single grain portions resulting in non-uniform drying. It is then of paramount importance to understand the physical phenomena that control the flow of grains in a mixed-flow dryer to guarantee their quality and minimize the risk of quality loss and waste of energy, thereby optimizing the process drying condition. With this objective, a two dimensional simulation model for the grain mass flow in a mixed-flow dryer based on Discrete Element Method (DEM) has been developed. The influences of the side walls and air ducts on solids mass flow were studied by evaluating the residence time distribution (RTD), particle velocity profiles and particle trajectories. The simulation results were validated with experiments using a semi-technical dryer test station with transparent Plexiglas front wall. The obtained results revealed the complexity of the drying process, the influences of the wall friction and half air ducts positioned directly on the wall on the bulk particle movement. Grains in mixed-flow dryers have different vertical velocities resulting in different residence times of every single portion of grains. The experimental validation confirms and verifies the DEM calculation ability for predicting particle flow.

K. L. Iroba · J. Mellmann (✉)
Department of Postharvest Technology, Leibniz-Institute for Agricultural Engineering Potsdam-Bornim (ATB), Max-Eyth-Allee 100, 14469 Potsdam, Germany
e-mail: jmellmann@atb-potsdam.de

F. Weigler · T. Metzger · E. Tsotsas
Faculty of Process and Systems Engineering, Thermal Process Engineering, Otto-von-Guericke University Magdeburg, Universitaetsplatz 2, 39106 Magdeburg, Germany

**Keywords** Mixed-flow dryer · Grain flow · Discrete element method · Particle velocity · Residence time

**List of symbols**

| | |
|---|---|
| $A$ | Cross-sectional area ($m^2$) |
| $d$ | Diameter (m) |
| $E$ | Modulus of elasticity ($N\,m^{-2}$) |
| $k$ | Stiffness ($N\,m^{-1}$) |
| $n$ | Total number of time intervals, see (2) |
| $N$ | Number |
| $\dot{N}$ | Dimensionless particle discharge rate |
| $P_n$ | Probability of tracer particles being discharged |
| $t$ | Time (s) |
| $\Delta t$ | Time interval (s) |
| $T_m$ | Mean residence time (s) |
| $x, y$ | Cartesian coordinates (m, m) |
| $\tau$ | Dimensionless time |

**Indices**

| | |
|---|---|
| $B$ | break-through |
| $cont$ | continuous |
| $i$ | current number of time interval |
| $m$ | mean |
| $n$ | normal |
| $P$ | particle |
| $s$ | shear |
| $st$ | step |
| $t$ | total |
| $TP$ | tracer particle |

## 1 Introduction

Grain drying is often conducted in continuous mixed-flow dryers (MFD) who are known for their high performance. It is well known that even small changes in grain properties or

process conditions for the drying of grains can have a great influence on its quality. Hence, the development of models to simulate and investigate the flow of grain is a topic of great relevance to post-harvest engineering. Concerning mixed-flow dryers, many papers are focused on how to increase the dryer performance and to save product quality, e. g. by improving the dryer control. Bruce [1] applied a multiple-bed computer simulation to model the dryer as a series of concurrent and counter-current elements. This model was successfully employed to predict the general behaviour of the dryer and the influence of operating variables on dryer performance. Different control strategies for mixed-flow dryers have been developed including model-based control, see for example [2–4]. The airflow patterns in MFD were experimentally investigated by Cenkowski et al. [5]. The authors discovered that about 30% of the dryer shaft volume operates in cross-flow configuration. Cao et al. [6] investigated the influence of the size and shape of air ducts, spacing between two air ducts, number of rows of air ducts and column height. They concluded that small air ducts are better than large air ducts, because the spacing between air ducts and effective bed depth are smaller for the small air ducts. Under the same height of dryer column the number of air ducts must be less for big air duct dryers. Therefore, with the increase in the air duct size the evaporation rate is decreased and the specific heat consumption is increased. Mellmann et al. [7] developed a model for the heat and mass transfer in MFDs which has been tested based on semi-technical experiments for the hot-air drying of wheat. For the grain mass flow, a simple plug-flow approach was adopted. Experimental investigations of the influence of air ducts and side walls on grain flow are reported by Kocsis et al. [8]. The authors measured the particle velocity profiles in different layers over the vertical dryer cross-section. The influence of the mentioned structural parameters on residence time distributions in this type of dryer has not been studied so far, however. Despite the above mentioned experimental investigations and some continuous models, there are still a number of problems associated with MFDs resulting in non-uniform moisture distribution of grains at the outlet.

DEM simulations are based on force balances with simple models of inter-particle forces. The motion of particles is modeled in a discrete way, described by Newton's laws on an individual particle scale [9]. The Discrete Element Method was introduced by Cundall [10] for the analysis of rock-mechanics problems and then applied to soils by Cundall and Strack [11]. The DEM has been used in different applications: flow and mixing of granular materials [12–15], packing structure, wall load, granular flow and combined heat transfer in silos and hoppers [16–18]. Also, DEM has been successfully applied to describe mixing of particles in rotary drums [19] and heat transfer from the wall in contact equipment [20].

The MFD is one of the most widely used grain dryers worldwide. Although it has been subject of much commercial development, there is no published report of application of discrete models, especially with the DEM to this dryer. Therefore, in the present work a two-dimensional simulation for the grain flow in a MFD was developed based on the DEM. To this purpose commercial software was applied [9]. The influences of air ducts and the side walls of the dryer on grain flow were investigated. To validate the model, experiments were conducted at the semi-technical dryer test station in Leibniz Institute of Agricultural Engineering Potsdam-Bornim (ATB), Germany, using wheat as the bed material.

## 2 Modes of operation

Industrial mixed-flow dryers are operated quasi-continuously in a record-by-record (interrupted) mode. During almost the whole drying time the grain bed is at rest while it is vertically moved only during ticks of time when the discharge device is opened. To batch-wise release the grain and to control the mass flow rate, different types of bottom discharge devices are used. Although mixed-flow dryers are operated in this interrupted mode, the flow behaviour of the grain through the dryer shaft can be investigated more favourably in the continuous flow mode [21]. This is the theoretical mode of operation where the discharge device is steadily opened and the grain flows out continuously. Hence, it was adopted for the DEM simulation.

## 3 Dem simulation and experimental investigation of particle flow

The DEM computes particle flow numerically by an explicit time integration scheme with suitable boundary and initial conditions. Here, the inter-particle force models are also applied to the interaction between a particle and a wall with the corresponding wall properties used. However, the wall is assumed to be so rigid that no displacement and movement result from this interaction. The dimensions of the simulated and experimental dryers are depicted in Figs. 1 and 2, respectively. The characteristics of bed material (moist wheat) used in the experiment are given in Table 1. In PFC-2D the damping coefficients are applied to the equations of motion in order to suppress the accelerating motion rather than velocity and absorb vibration energy, therefore, reaching mechanical equilibrium in a minimum number of cycles [9]. When a dynamic simulation of compact assemblies is required, the local damping coefficient should be set to a low value appropriate to energy dissipation of dynamic waves. For problems involving free flight of particles and/or impacts between particles, local damping is inappropriate. Hence, the local

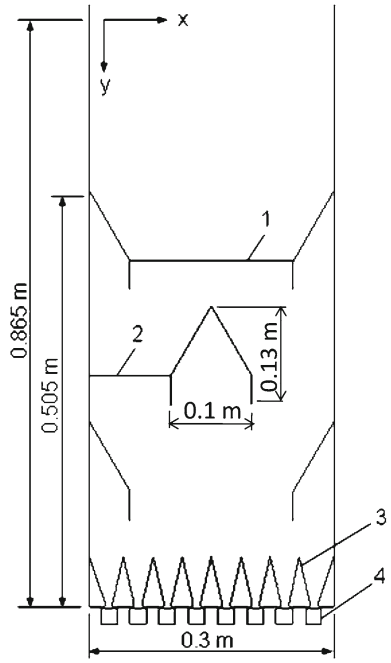


**Fig. 1** Schematic of the simulated dryer. 1, 2—Layers where particle velocities were monitored. 3, 4—Fixed and moving parts of bottom discharge device, respectively

damping coefficient was set to zero and viscous contact damping was used.

The actual shape of wheat is nearly ellipsoidal. This particle shape was used by Markauskas et al. [22] to simulate the piling problem. The authors adopted a multi-sphere model to compose ellipsoidal particles. However, multi-sphere model results in an increase in the number of particles with longer simulation time, while non-spherical particles requires more advanced algorithms and are more difficult to model [23]. Hence, mono-sized spherical particles were used for the simulation. In this work, the linear contact model was applied because it is the easiest, simplest and fastest contact model. Thus, normal stiffness $k_n$ and shear stiffness $k_s$ was set equal to each other according to Itasca [9]. The particle size used is big enough, so that van der Waals forces play no role. The $k_n$ and $k_s$ values were obtained as [24]

$$k_n = k_s = \frac{E \cdot A_P}{d_P} \tag{1}$$

where $A_p$ is the particle cross-sectional area ($m^2$), $E$ is modulus of elasticity ($N\,m^{-2}$), and $d_p$ is particle diameter. The mean equivalent spherical particle diameter and the bulk

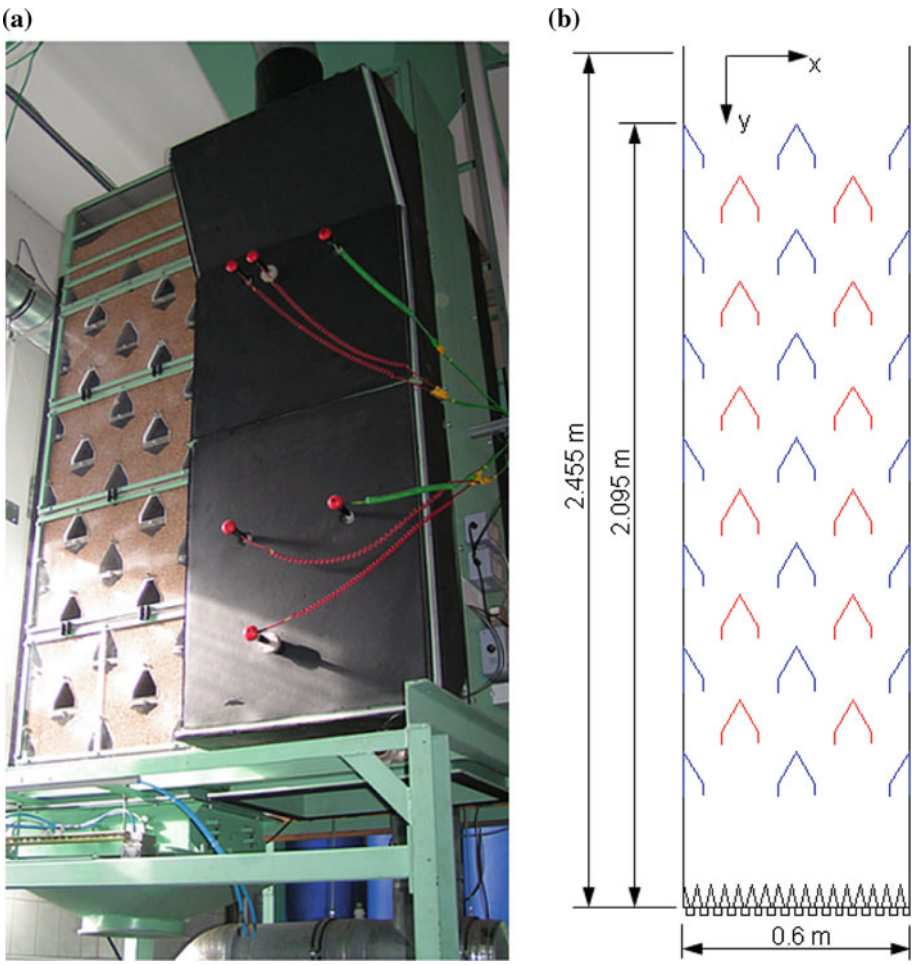


**Fig. 2** Photograph (**a**) and schematic diagram (**b**) of the pilot-scale MFD test station

**Table 1** Characteristics of the bed material (wheat) and process parameters used in the simulation

| Characteristic / parameter | Symbol | Unit | Value | Ref. |
|---|---|---|---|---|
| Mean particle diameter particle shape: spherical | $d_P$ | m | 0.0042 | |
| Particle density | $\rho_p$ | $\mathrm{kg\,m^{-3}}$ | 1300 | [25] |
| Gravitational acceleration | $g$ | $\mathrm{m\,s^{-2}}$ | 9.81 | |
| Particle friction coefficient | $\mu_P$ | | 0.433 | [26] |
| Wall friction coefficient | $\mu_W$ | | 0.364 | [27] |
| Modulus of elasticity | $E$ | $\mathrm{N\,m^{-2}}$ | $3.31 \times 10^9$ | [26] |
| Normal stiffness | $k_n$ | $\mathrm{N\,m^{-1}}$ | $1.83 \times 10^5$ | |
| Shear stiffness | $k_s$ | $\mathrm{N\,m^{-1}}$ | $1.83 \times 10^5$ | |
| Time step | $\Delta t_{st}$ | s | $4.508 \times 10^{-6}$ | |
| Local damping coefficient | $l_d$ | | 0.0 | |
| Viscous damping coefficient, normal | $v_n$ | | 0.9 | |
| Viscous damping coefficient, shear | $v_s$ | | 0.9 | |
| Number of particles generated | $N_P$ | | 39,000 | |

density of wheat were obtained from own measurements, the other properties were taken from literature [25–27].

Table 1 Characteristics of the bed material (wheat) and process parameters used in the simulation.

The assumptions involved in the simulation of the particle flow can be summarized as follows:

1. The geometry of the dryer is constant over the depth, hence, two-dimensional model was adopted.
2. The dryer geometry simulated comprises 1/2 of the width of the test dryer.
3. The length of flow in the simulation is about 1/4 of the length of flow in the experiment, see Figs. 1 and 2.
4. The single wheat grain is modeled as a spherically shaped particle.
5. The continuous flow case is considered.
6. It is assumed that there is no air flow.

Only a part of the real dryer geometry was modeled in order to save computational time. The computational domain is placed above the discharge device. The cross-sections of the air ducts and the bottom discharge device are consistent with the real dimensions of the test dryer. In the simulation three parameters were investigated: the particle vertical velocities, the residence time and the trajectories of the particles. The simulation conditions are the same for these three parameters except that the tracer particles were not considered for the velocity profile investigations.

## 3.1 Particle velocity profiles

### *3.1.1 Simulation*

At first, the described two-dimensional dryer geometry was implemented. A simulation was started with the random numerical generation of particles without overlaps at the top of the dryer, followed by gravitational settling to form a random packing. Thereafter, the bottom discharge device was opened with a speed of $0.1\,\mathrm{m\,s^{-1}}$ which corresponds to the speed of the moving part of the test station discharge device. Due to the assumed spherical shape of particles, bridging occurred at the bottom discharge device. However, bridging did not occur at the test dryer. This is due to the ellipsoidal shape of the wheat grains flowing lengthwise through the bottom discharge device where the smaller grain diameter is active. To avoid bridge formation in the simulation, the fixed part of the discharge device was set into vibration ($4\,\mathrm{m\,s^{-1}}$ over a distance of 0.000002 m). This imitates the realistic behaviour of the discharge device of the MFD test station during operation. A time of 0.113 s was left to elapse for the particles to attain steady state outflow from the dryer before monitoring the velocities. The velocity distributions were then calculated at two different layers of the vertical dryer cross section, these layers were discretized into units of $\Delta x = 1\,\mathrm{cm}$ in the horizontal. The results are shown in Fig. 3. The particles are continuously refilled and allowed to settle by acceleration due to gravity, 1,000 particles were generated every 0.375 s throughout the simulation.

### *3.1.2 Experiment*

The experimental investigation of particle flow was conducted using the MFD test station. The front wall of the grain flow study equipment is made of transparent acrylic glass (Fig. 2) so that the movement of the particles can be optically observed. At the lower end a pneumatically operated slide bottom discharge device is employed. All experiments have been conducted with moist wheat as bed material with an average moisture content of about 18% w.b. (wet basis) and a bulk density of $783\,\mathrm{kg\,m^{-3}}$. To measure the particle velocity profiles a digital video camera was employed. The video was evaluated with video and picture software Adobe

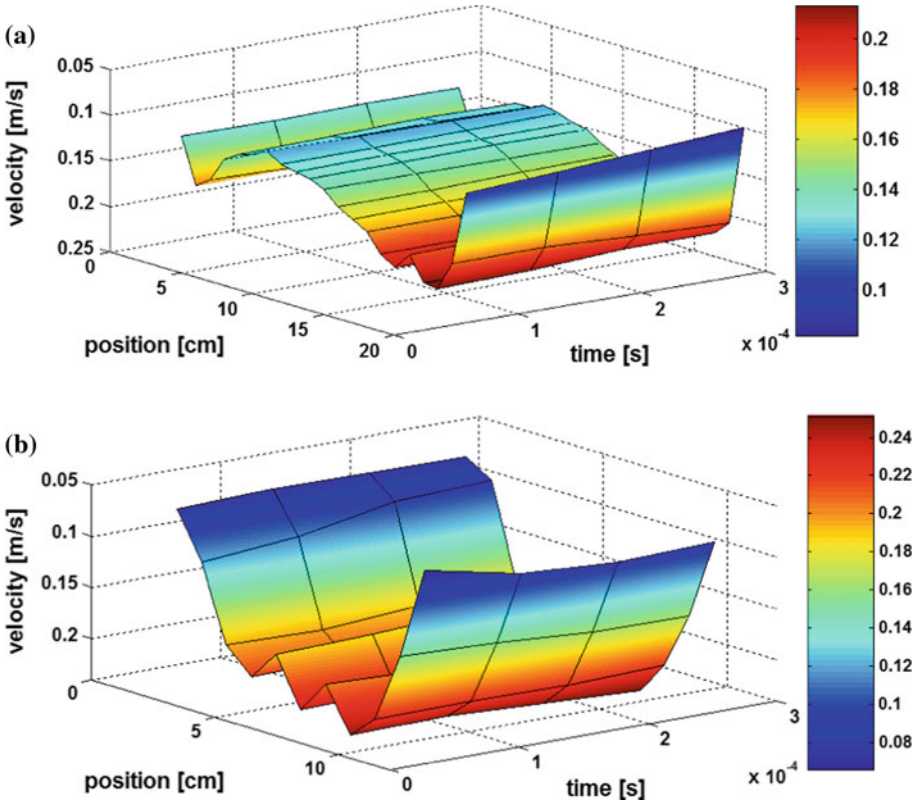


**Fig. 3** Particle velocity profiles calculated from simulation: **a** layer 1, *centre*; **b** layer 2, *left* (see Fig. 1)

Premiere (version 6.5). This software records pictures at a rate of 30 pictures per second. The velocity distributions were determined at different layers over the entire cross-section in order to measure the complex grain flow in the dryer. As these measurements revealed there is a nearly symmetric flow profile over the width related to the vertical center line of the dryer [8]. This makes clear that the friction effects are almost the same at both side walls. For comparison with the simulated results, hence, two layers have been selected close to the discharge device: one central layer between two air ducts and one layer between the left side wall and the adjacent air duct. For accurate and proper evaluation of the particle velocities through the transparent acrylic glass front wall, these layers were divided in the same manner like in the simulation. The paths of the particles were followed over a vertical distance of $\Delta y = 5\,\mathrm{cm}$.

The computational and experimental results obtained from the particle velocity investigations revealed that wall friction and the air ducts play an important role in the flow pattern of grains in MFDs, with a large effect on the bulk particle movement. As Figs. 3 and 4 show, the results obtained are qualitatively similar and Fig. 5 shows comparison between the simulation and experimental velocity profiles. However, the vibration implemented in the simulation to avoid bridge formation plays a significant role, because it affects the particle-particle and particle-wall interactions with a trend towards increased particle velocities. Grains in the center of the dryer have relatively high velocities and are delivered

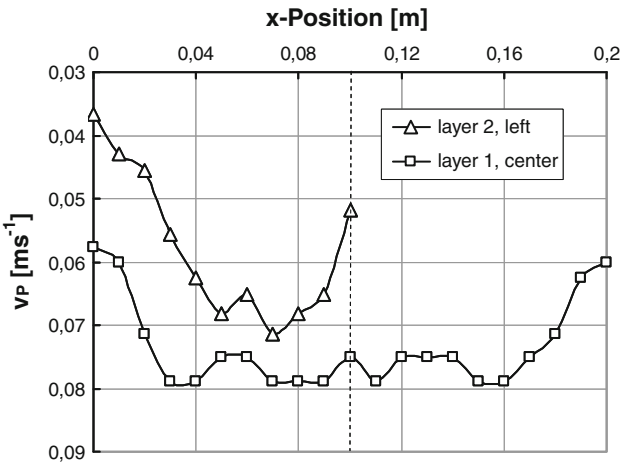


**Fig. 4** Experimental velocity profiles

faster while grains close to the side walls have reduced velocities because of wall friction. The effect of the full central air duct can be seen in Figs. 3a and 4 (layer 1, center). This air duct reduces the vertical velocity of particles that flow directly above its tip. Figures 3b and 4 (layer 2, left) show the particle velocity profiles between side wall and full central air duct. Higher velocities are obtained in the center of the respective gap with small fluctuations resulting from the half air duct below layer 2 and also from the fixed part of the bottom discharge device. The half air ducts at the side walls pose the largest obstruction to the free flow of grains. Particles

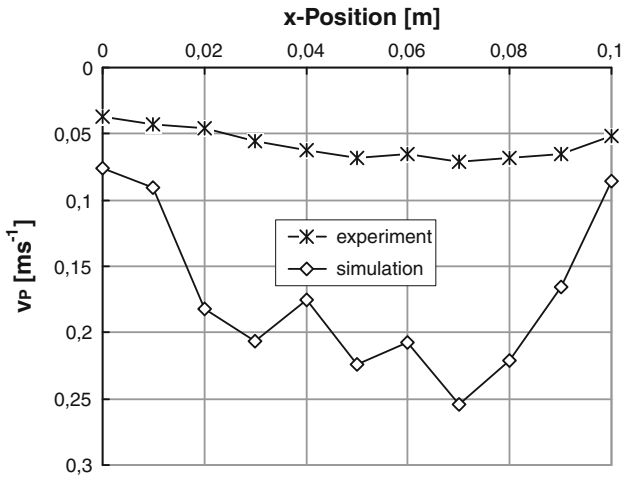


**Fig. 5** Comparison of particle velocities obtained from simulation and experiment in layer 2, *left*

that flow close to the side walls are displaced towards the side walls by particles that flow through the center. Hence, these particles reside in respective corners (between two half air ducts) for longer time than necessary. It, therefore, becomes evident that every single grain in a MFD has no uniform vertical velocities as they flow down the dryer resulting to different residence times.

## 3.2 Residence time distribution

The differences in particle movement between the near-wall and central regions have been further investigated by determining the RTD in the dryer with the help of tracer particles, which were introduced at the top of the equipment. This is because the residence time of the particles as they flow down the dryer is a function of their positions over the width of the dryer.

### *3.2.1 Simulation*

In the RTD simulation, 400 mono-dispersed yellow colored grains were generated and used as tracer particles. The geometry of the dryer employed and the layer of yellow tracer particles at the beginning of the RTD simulation are shown in Fig. 6a. To save computational time, any particle that was discharged from the dryer was deleted. The length of flow of the tracer particles amounts to 0.505 m. This corresponds to about 1/4 of the length of flow of the tracer particles in the test dryer. The whole simulation lasted for 7.36 s. The histories of the y-positions with time of the tracer particles were monitored. The number of particles deleted and the time it took for each of them to travel from the top lattice position to the bottom of the dryer were monitored and computed, respectively. This time corresponds to the residence time of the yellow tracer particles. The graphical representation of the calculated residence time distribution is given in Fig. 8 with dimensionless axes. The break-through time $t_B$ of the tracer particles was at 2.25 s. This is the time the first tracer particle leaves the dryer. At the end of the simulation, 99% (396) of the yellow particles used for residence time calculation were recovered from the dryer while 1% (which represents four particles) was left in the dryer.

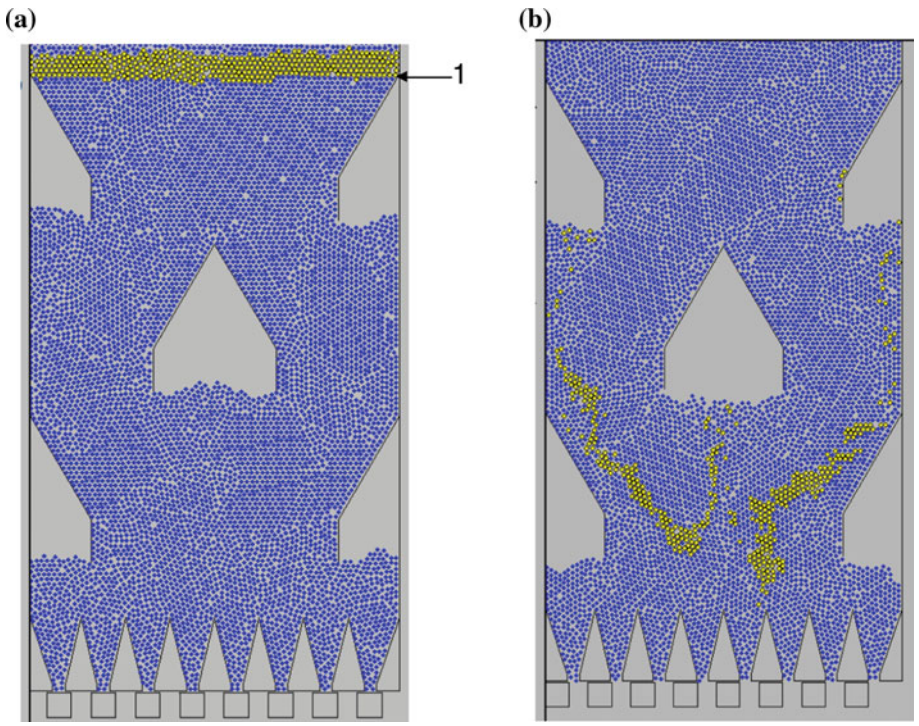


**Fig. 6** **a** Layer of tracer particles at the beginning of the RTD simulation: 1—Starting position of tracer particle layer. **b** Deformation of the tracer particles stripe in the course of the simulation

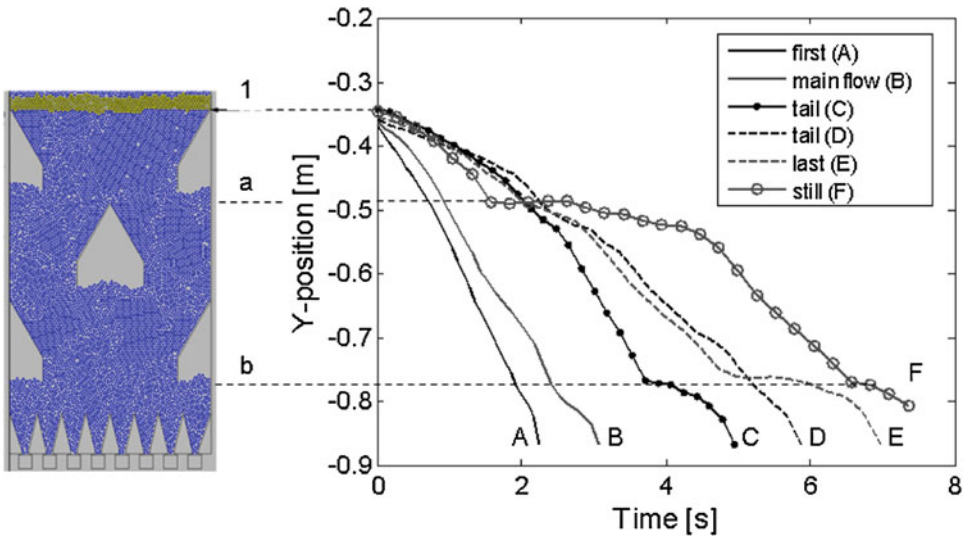


**Fig. 7** Calculated vertical trajectories of selected tracer particles: *A* first set of tracer particles leaving the dryer. *B* tracer particles discharged at about $T_m$.*C*, *D*, *E* = contributors to the long tail of the RTD. *F* tracer particles still in the dryer at the end of the simulation. *1* starting position of tracer particle layer. *a, b* inflection points due to flow obstacles under the half air ducts

$$T_m = \frac{\sum_{i=1}^{n} N_{TP} \cdot t_i \cdot \Delta t}{\sum_{i=1}^{n} N_{TP,i} \cdot \Delta t} \tag{2}$$

The mean residence time, $T_m$ was calculated with a time class interval ($\Delta t$) of 0.10 s using (2), resulting in a value of $T_m$ = 2.97 s. $N_{TP}$ is the number of tracer particles discharged at a particular time ($t$).

### 3.2.2 Particle trajectories

To further study the flow behavior of discrete particles, the trajectories of the 400 yellow tracer particles were monitored during the simulation. The starting point of the tracer particles corresponds to position 1 depicted in Fig. 6a. This is where the tracer particles were positioned at the beginning of the simulation. The trajectories of selected tracer particles are presented in Fig. 7. The first trajectory (A) represents the set of particles that first leave the dryer. From the plot, it can be seen that these tracer particles move down the dryer with low friction effect and obstruction from the air ducts and side walls. This trajectory depicts the breakthrough time, which is the time the first tracer particle leaves the dryer. The second trajectory (B) indicates particles that leave the dryer almost at the same time as the calculated mean residence time. Trajectories (A) and (B) represent particles that flow through the center of the dryer (main flow) with relatively high velocity. The next three trajectories (C, D, and E) characterize the flow of particles that contribute to the long tail of the RTD, see Fig. 8. Trajectory (E) shows the last tracer particle that left the dryer during the simulation. The trajectory (F) illustrates the flow behavior of tracer particles that have not left the dryer before the simulation ended. The trajectories C-F depict tracer particles that experience a lot of hindrances and obstructions in the dryer

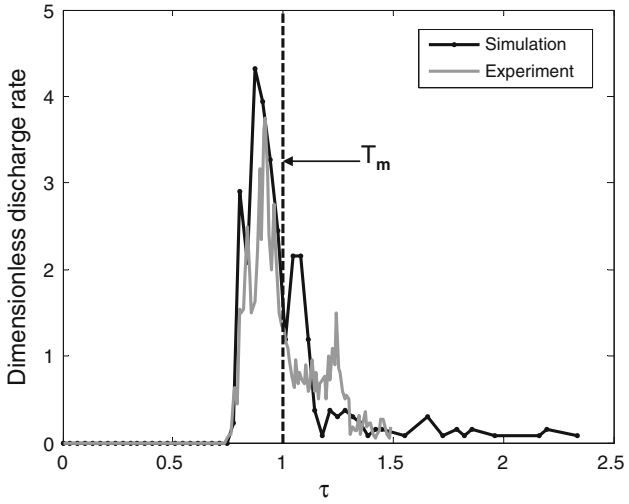


**Fig. 8** Comparison between simulated and experimental RTD

caused by friction effects, side walls and air ducts, so that they need a longer time to travel down the dryer. As can be seen from Fig. 7, these trajectories show two significant inflection points due to the influence of the half air ducts. These inflection points located at about $y = -0.49$ m (position a) and $y = -0.78$ m (position b) correspond exactly to the positions of the lower ends of the half air ducts, see Fig. 7, left ($y = 0$ represents the position where the particles were generated in the simulation). As could be well observed both in experiment and in the simulation (video), particularly the corners under the half air ducts posed dead zones to the particle flow where the tracer particles resided extremely long. This flow pattern results from horizontal displacement of grains towards the side walls by the main flow through the center of the dryer thereby increasing the wall friction.

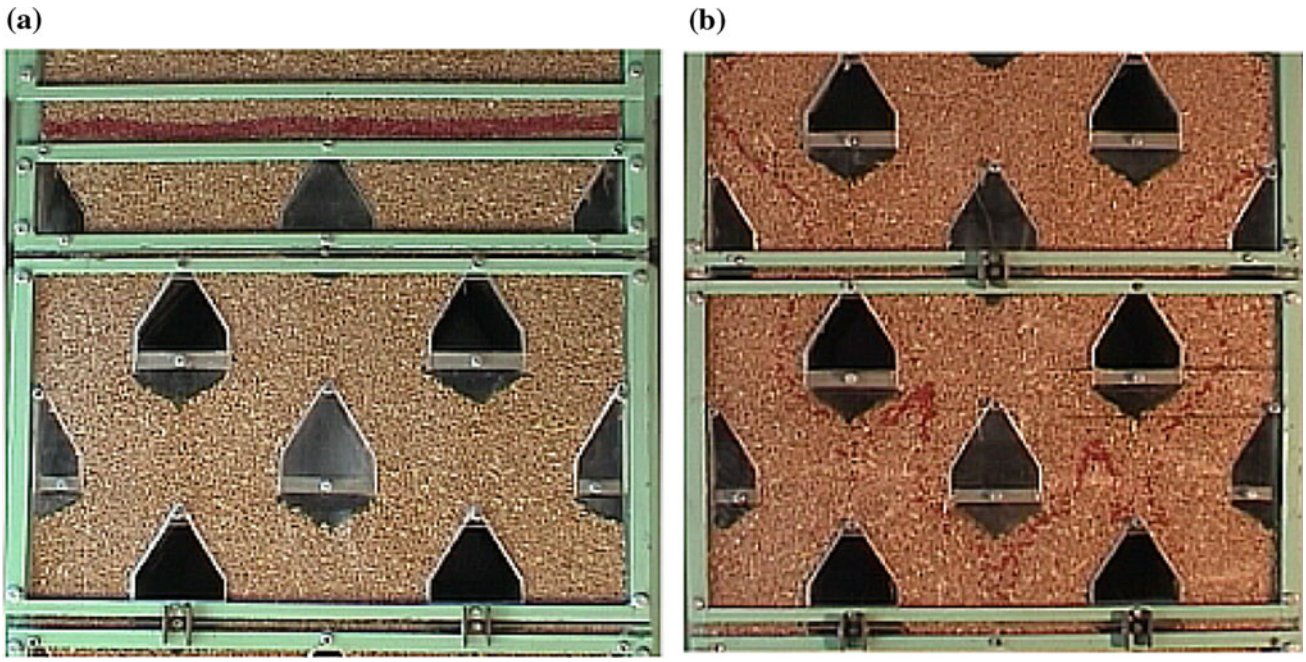


**Fig. 9** **a** Layer of *red* colored tracer particles at its starting position. **b** Flow pattern of the tracer particles

*3.2.3 Experiment*

To measure the residence time, 2,400 colored wheat grains were used as tracer particles. The tracer particle layer was visible at the front of the dryer. The residence time distribution was measured by counting the colored particles in the discharged grain samples. The experiment was recorded using the above mentioned digital video camera. As can be seen from Fig. 9 (a & b), the initial distribution and the flow pattern of the colored grains are shown, respectively. The discharged mass of grains per loop was always weighed with a balance and the numbers of tracer particles in each discharge sample were carefully counted by spreading each sample on a wide flat tray. The discharge continued in this sequence of single loops until about 73% of the tracer particles had left the dryer after 18 h experimental time. Throughout the experiment the dryer was continuously refilled. In this manner the RTD has been measured as shown in Fig. 8. The break-through time $t_B$ of the yellow tracer particles was at 24.3 s. Using (2) with a time class interval ($\Delta t$) of 0.30 s, the mean residence time $T_m$ was determined to be 32.6 s. It was computed only for the 73% discharged colored tracer particles (in total 1,756) that were collected from the discharge samples. The remaining 27% (644) were trapped at the side walls of the dryer between the half air ducts (corners). The present design of MFDs creates corners at the side walls between the half air ducts positioned directly at the side walls. Particles are trapped and reside in these corners for a long time. As a result, they are delivered with significant delay at the discharge, which can lead to excessive over-drying and loss of product quality. It should be noted that after the experiment the dryer was emptied and during this stepwise discharge, colored grains were still found even in the last discharged portion.

For the purpose of direct comparison of the residence time distributions obtained from simulation and experiment their coordinates are transformed into dimensionless discharge rate and time. The dimensionless time ($\tau$) of the particle flow was obtained by dividing the actual times $t$ by the corresponding mean residence times $T_m$ as

$$\tau = \frac{t}{T_m} \tag{3}$$

The dimensionless discharge rate of tracer particles $\dot{N}_{TP}$ is given by

$$\dot{N}_{TP} = \frac{P_n}{\Delta\tau} = \frac{N_{TP,i} \cdot T_m}{N_{TP,t} \cdot \Delta t} \tag{4}$$

where $P_n$ is the probability of tracer particles being discharged

$$P_n = \frac{N_{TP,i}}{N_{TP,t}} \tag{5}$$

The term $N_{TP,i}$ represents the number of tracer particles discharged per time interval $\Delta t$ and $N_{TP,t}$ the total number of tracer particles discharged. The dimensionless time interval $\Delta\tau$ can be written as

$$\Delta\tau = \frac{\Delta t}{T_m} \tag{6}$$

As is clear from the graphs in Fig. 8, the measured and calculated dimensionless residence time distributions are in good agreement. The flow profiles of particles in the simulation and in the experiment are consistently similar. The peaks represent the tracer particles that flow through the center of the dryer with higher particle velocities and lower friction effect. The long tails revealed the influence of wall friction and the half air ducts positioned directly at the side walls on the grain flow. These particles travel with lower vertical velocities due to higher frictional effects. As a result, grains have different residence times in the dryer. The consequence of this is that an uneven moisture distribution will result from drying, with the risk of product quality loss during subsequent storage. Grains with higher velocities may be under-dried and those with lower velocities may be over-dried depending on the required drying time. If the residence time of the grains is less than the drying time, then under-drying occurs, and if the residence time of the grains is higher than the drying time the grains will be over-dried. Over-drying is costly in three ways:

- There is excessive shrink, and less weight is sent to the market;
- There is extra drying cost (energy) for removing too much moisture;
- Thermal damages may occur.

Under-drying can cause the formation of mould and toxins during subsequent storage. The tail of the RTD for the simulation is longer than that for the experiment because 99% of the tracer particles were recovered from the simulation and only 73% from the experiment. This means that if more than 73% were collected and evaluated, then the trapped 27% tracer particles would have prolonged the tail for the experiment.

## 4 Conclusion

Residence time and particle velocity distributions were investigated in order to better understand the physical phenomena that control the particle flow in MFDs. The comparison between simulated and experimental results revealed that the DEM can adequately predict the main features of particle flow. A 2-D DEM model and commercial software have been employed in the present work to study the flow behavior at the particle scale. The results obtained show that two regions exist in MFDs, the near wall region with low particle velocity, and the central region with high particle velocity. Wall friction has a large effect on the bulk particle movement. Wall friction dominates in the near wall region whereas particle-particle forces are dominant in the central region. Thus, grains in MFDs have different vertical velocities, resulting in different residence times. The half air ducts pose an obstruction to the free flow of grains. It is expected that this behavior can lead to the following consequences in case of drying operation:

- A broad moisture content distribution at the outlet (inhomogeneous drying) with the risk of product quality loss during subsequent storage;
- Extra drying costs (energy) for removing too much moisture.

In general, the analysis shows that the present design of MFDs does not provide an adequate amount of cross-mixing. Therefore, the future goal will be to develop new, better designs of MFDs. 2-D DEM can be used to this purpose, since it has shown to properly capture all flow patterns and residence time distributions which are important for product quality, however with over prediction of the velocity profiles. 2-D DEM does not predict accurately the absolute values of particle velocity, which may be due to the vibration imposed on the bottom discharge device and the spherical particle shape used in the simulation. Therefore, optimization of the process is required in the subsequent studies. Application of a more realistic ellipsoidal particle shape and multi-sphere model will be considered. Additionally, air flow, heat and mass transfer, which have all been neglected in the present preliminary work, should be implemented.

**Acknowledgments** The authors are grateful to the German Federal Ministry for Education and Research for the financial support (BMBF/PTJ Project No. 0339992A, TP1.3)

## References

1. Bruce, D.M.: Simulation of multiple-bed concurrent-, counter-, and mixed-flow grain driers. J. Agric. Eng. Res. **30**, 361–372 (1984)
2. Courtois, F., Abud Archila, M., Bonazzi, C., Meot, J.M., Trystram, G.: Modeling and control of a mixed-flow rice dryer with emphasis on breakage quality. J. Food Eng. **49**, 303–309 (2001)
3. Liu, H., Zhang, J., Tang, X., Lu, Y.: Fuzzy control of mixed-flow grain dryer. Dry. Technol. **21**, 807–819 (2003)
4. Liu, X., Chen, X., Wu, W., Zhang, Y.: Process control based on principal component analysis for maize drying. Food Control **17**, 894–899 (2006)
5. Cenkowski, S., Miketinac, M., Kelm, A.: Airflow patterns in a mixed-flow dryer. J. Can. Agric. Eng. **32**, 85–90 (1990)
6. Cao, C.W., Yang, D.Y., Liu, Q.: Research on modeling and simulation of mixed-flow grain dryer. Dry. Technol. **25**, 681–687 (2007)
7. Mellmann, J., Richter, I.-G., Maltry, W.: Experiments on hot-air drying of wheat in a semi-technical mixed-flow dryer. Dry. Technol. **25**, 1287–1295 (2007)
8. Kocsis, L., Teodorov, T., Mellmann, J., Gottschalk, K., Mészáros, C., Farkas, I.: Analysis of grain flow experiments in a mixed-flow grain dryer. In: Proceedings of the 17th World Congress of International Federation of Automatic Control (IFAC), pp. 1608–1612. Seoul, Korea, 6–11 July (2008)

9. Itasca Consulting Group, Inc.: PFC 2D, Version 3.1, Theory and Background Manual. Minneapolis, USA (2004)
10. Cundall, P.A.: A computer model for simulating progressive large scale movements in blocky rock systems. In: Proceedings of the Symposium of the International Society of Rock Mechanics, vol. 1, Paper No. II-8. Nancy, France (1971)
11. Cundall, P.A., Strack, O.D.: A discrete numerical model for granular assemblies. Geotechnique **29**, 47–65 (1979)
12. Mankoc, C., Janda, A., Arévalo, R., Pastor, J.M., Zuriguel, I., Garcimartín, A., Maza, D.: The flow rate of granular materials through an orifice. Granular Matter **9**, 407–414 (2007)
13. Teufelsbauer, H., Wang, Y., Chiou, M.-C., Wu, W.: Flow-obstacle interaction in rapid granular avalanches: DEM simulation and comparison with experiment. Granular Matter **11**, 209–220 (2009)
14. Bertrand, F., Leclaire, L., Levecque, G.: DEM-based models for the mixing of granular materials. Chem. Eng. Sci. **60**, 2517–2531 (2005)
15. Stewart, R., Bridgwater, J., Zhou, Y., Yu, A.: Simulated and measured flow of granules in bladed mixer—a detailed comparison. Chem. Eng. Sci. **56**, 5457–5471 (2001)
16. Sykut, J., Molenda, M., Horabik, J.: DEM simulation of the packing structure and wall load in a 2-dimensional silo. Granular Matter **10**, 273–278 (2008)
17. Langston, P.A., Matchett, A.J., Fraige, F.Y., Dodds, J.: Vibration induced flow in hoppers: continuum and DEM model approaches. Granular Matter **11**, 99–113 (2009)
18. Kruggel-Emden, H., Wirtz, S., Simsek, E., Scherer, V.: Modeling of granular flow and combined heat transfer in hoppers by discrete element method. J. Press. Vessel Technol. **128**, 439–444 (2006)
19. Kwapinska, M., Saage, G., Tsostas, E.: Mixing of particles in rotary drums: a comparison of discrete element simulations with experimental results and penetration models for thermal processes. Powder Technol. **161**, 69–78 (2006)
20. Tsostas, E., Kwapinska, M., Saage, G.: Modeling of contact dryers. Dry. Technol. **25**, 1377–1391 (2007)
21. Iroba, K.L., Weigler, F., Mellmann, J., Metzger, T., Tsotsas, E.: Residence time distribution in mixed-flow grain dryers. Dry. Technol. **28** (2010), in press
22. Markauskas, D., Kačianauskas, R., Džiugys, A., Navakas, R.: Investigation of adequacy of multi-sphere approximation of elliptical particles for DEM simulations. Granular Matter **12**, 107–123 (2010)
23. Luding, S.: Cohesive, frictional powders: contact models for tension. Granular Matter **10**, 235–246 (2008)
24. Itasca Consulting Group, Inc.: PFC 2D, Version 3.1, Augmented Fishtank, Minneapolis, USA (2004)
25. Sokhansanj, S., Lang, W.: Prediction of kernel and bulk volume of wheat and canola during adsorption and desorption. J. Agric. Eng. Res. **63**, 129–136 (1996)
26. Mohsenin, N.N.: Physical Properties of Plants and Animal Materials, Vol. 1. Gordon and Breach Science Publishers Inc, New-York (1970)
27. Kunibert, M.: Transport, Umschlag, Lagerung in der Landwirtschaft. VEB Verlag Technik, Berlin (1983)